

pH-responsive protein microcapsules fabricated via glutaraldehyde mediated covalent layer-by-layer assembly

Weijun Tong · Changyou Gao · Helmuth Möhwald

Received: 21 March 2008 / Revised: 28 April 2008 / Accepted: 6 May 2008 / Published online: 1 June 2008

© The Author(s) 2008

Abstract Bovine serum albumin (BSA) hollow microcapsules were fabricated through glutaraldehyde (GA) mediated covalent layer-by-layer assembly. The GA cross-linking of the adsorbed BSA on the colloidal particles enabled their surfaces to be covered by reactive aldehyde groups, which reacted with BSA molecules to result in another covalently linked layer. Repeating of this cycle could then yield particles coated with BSA multilayers. Hollow microcapsules well dispersed in water were obtained after core removal. The good integrity and morphology of the BSA capsules were confirmed and characterized by confocal laser scanning microscopy, scanning electron microscopy and scanning force microscopy. The obtained BSA microcapsules possess reversible pH response, i.e., the capsules are permeable to macromolecules below pH 4 or above pH 10, while impermeable in between. The mechanisms of permeability transition were discussed. Using this property, dextran, with a molecular weight of ~155 kDa, was successfully loaded.

Keywords Bovine serum albumin · Glutaraldehyde · Covalent layer-by-layer · pH-responsive · Microcapsules

Introduction

Protein nano-/microspheres and capsules for controlled and/or sustained release have attracted considerable attention for pharmaceutical and other applications [1–9]. As natural biomacromolecules, proteins are generally considered to be biocompatible and biodegradable. Most previous studies focused on different kinds of albumins [1–3], milk protein caseins [4–7], as well as whey proteins [8, 9], because they are abundant in nature and inexpensive. The most frequently employed procedure for fabricating the protein microspheres is as follows. An aqueous solution of proteins which may contain drugs is dispersed in an organic phase to form a reverse emulsion. Then cross-linking of the droplets is conducted to stabilize the structure, resulting in the microspheres [3]. Although the droplet size of the emulsion, and thus the resulting microsphere size, is determined by the nature of the dispersion, the spheres with smaller size and narrower size distribution are difficult to obtain. By other methods such as desolvation of the protein solution followed by cross-linking [10] or electrospray drying [11], protein nanoparticles can be fabricated.

Compared with spheres, hollow protein capsules have larger capacity to load desired substances. Several approaches have been developed to fabricate hollow protein capsules. For example, bovine serum albumin (BSA) capsules with disulfide cross-linked shells of ~50 nm and cores containing air or non-aqueous liquid were prepared using ultrasonic emulsification [12, 13]. In another case, the hollow protein capsules with a size of tens of microns were fabricated through protein adsorption on the pendent organic droplets followed by evaporation of the organic solvent [14]. However, the above-mentioned methods are not applicable for fabricating capsules with defined size, wall thickness and compositions. More recently, a new

W. Tong · C. Gao (✉)

Key Laboratory of Macromolecular Synthesis and Functionalization, Ministry of Education, Department of Polymer Science and Engineering, Zhejiang University, Hangzhou 310027, China
e-mail: cygao@mail.hz.zj.cn

W. Tong · H. Möhwald

Max-Planck-Institute of Colloids and Interfaces, 14424 Potsdam, Germany

method combining colloidal templating and layer-by-layer (LbL) assembly [15, 16], followed by core removal, produces hollow microcapsules with precisely controlled structures and properties [17–19]. Of special interest is that it is possible to tune the stimuli-responsive properties of the capsule by incorporation of functional molecules into their wall or interior, thus the loading and subsequent release of diverse substances into/from the microcapsules can be controlled in a desired manner. By this method, the hollow microcapsules with proteins or enzymes as one of the wall compositions also have been obtained [20–23]. But in most of the cases, the capsule walls are based on the electrostatic interaction.

Glutaraldehyde (GA) is most widely used as a cross-linking reagent for preparation of protein spheres and capsules because its aldehyde groups can easily react with amine groups at mild conditions. In our previous studies, GA was used to cross-link polyelectrolyte microcapsules to manipulate their properties [24, 25]. More recently, we developed a GA-mediated covalent layer-by-layer assembly method to fabricate single component polyelectrolyte microcapsules [26, 27]. Hemoglobin capsules and nanotubes with retained activity were fabricated in a similar way [28, 29]. The single component polyelectrolyte microcapsules are robust and their properties can be controlled by the molecular weight of used polyelectrolyte [26, 27]. However, due to the high cross-linking density the capsules lost their stimuli-response.

BSA has a high content of charged residues of amino acids, such as aspartic and glutamic acids, lysine, and arginine [30, 31]. GA only cross-links the amine group of lysine [32], while the other charged residues of amino acids still exist. Consequently, pH response of the resultant products can be expected. Moreover, previous studies have shown that the GA-cross-linked albumin microspheres are relatively non-immunogenic and biodegradable in muscle without adverse tissue reactions [2]. Therefore, the GA cross-linked BSA spheres/capsules are promising for pharmaceutical applications. Herein, we describe the preparation of BSA microcapsules fabricated in a covalent layer-by-layer assembly manner through GA cross-linking. In this approach, BSA is first assembled on the surfaces of the colloidal templates. Then the coated particles are suspended in GA solution to cross-link the adsorbed BSA layer and activate the surface for the next covalent assembly of BSA. This procedure is repeated several times until the desired layer number is reached. Hollow capsules are obtained by removal of the cores. The microstructure of the obtained BSA microcapsules is investigated by confocal laser scanning microscopy (CLSM), scanning electron microscopy (SEM) and scanning force microscopy (SFM). The capsules show reversible pH-controlled permeability, which can be used to encapsulate macromolecules. The possible mechanisms of pH response are discussed.

Experimental section

Materials

BSA, tetramethylrhodamine isothiocyanate labeled dextran (TRITC-dextran, $M_w \sim 155$ kDa), rhodamine 6G (Rd6G), manganese sulfate hydrate ($MnSO_4 \cdot H_2O$), disodium ethylenediaminetetraacetate dihydrate (EDTA), ammoniumhydrogencarbonate (NH_4HCO_3) and glutaraldehyde (GA, 50 wt.% solution in water) were all obtained from Sigma-Aldrich. All the chemicals were used as received. The water used in all the experiments was prepared in a three-stage Millipore Milli-Q Plus 185 purification system and had a resistivity higher than 18.2 M Ω . Spherical $MnCO_3$ microparticles with an average diameter of 7.4 ± 0.4 μm were synthesized according to literature by mixing $MnSO_4$ and NH_4HCO_3 solutions [33, 34].

Methods

Multilayer build-up onto planar substrate

Silicon wafers were treated with H_2O_2/H_2SO_4 (30/70 v/v) solution for 1 h and thoroughly rinsed with water. The pre-treated substrates were sequentially immersed into BSA (4 mg/ml, in 0.5 M NaCl, pH=4.7) and GA solutions (2%) for 30 min, with three water rinses at each interval. After each BSA assembly, the surface water of the multilayer was blown away by flowing nitrogen and the thickness of the film was measured immediately by ellipsometry.

Fabrication of hollow protein microcapsules

BSA was adsorbed onto the $MnCO_3$ microparticles under the same conditions employed for its multilayer construction on planar substrate. After BSA adsorption, the excess proteins were removed by centrifugation at $300 \times g$ for 5 min, and the coated particles were washed three times with water. Then the particles were dispersed in the GA solution for 30 min, followed by three washings. The cross-linked and surface activated particles were dispersed in the protein solution again. This procedure was repeated until ten BSA layers were assembled. The coated particles were further cross-linked with 2% GA solution for 12 h to stabilize the structure. After washing with water five times, the coated particles were incubated in 0.1 M HCl solution for 30 min under continuous shaking to remove the cores. The resultant capsules were washed three times with 0.01 M EDTA solution to rinse off the Mn^{2+} . Finally, the capsules were washed three times with water and dispersed in water.

Ellipsometry

Ellipsometry was performed using an optical null ellipsometer (Multiskop Ellipsometer, Optrel GmbH) with a He–Ne laser at 632.8 nm at an angle of 70°. Silicon wafers were used as the substrates for the multilayer formation and were cleaned as described above. A refractive index value of 1.32 for BSA multilayer was measured from ten-layer film and used for all the calculations. Each point was averaged from ten individual measurements.

Confocal laser scanning microscopy (CLSM)

Confocal images were taken with a Leica confocal scanning system mounted to a Leica Aristoplan and equipped with a 100× oil immersion objective with a numerical aperture (NA) of 1.4. For visualization, Rd6G was used to stain the BSA capsules. To investigate the permeability, a drop of the capsule suspension was mixed with the fluorescent probes solution with same pH and observed after 30 min.

Scanning electron microscopy (SEM)

Samples were prepared by applying a drop of the capsule suspension onto glass slides. After dried overnight, the samples were sputtered with gold and measured by a Gemini Leo 1550 instrument at an operation voltage of 3 keV.

Scanning force microscopy (SFM)

A drop of the sample suspension was applied onto freshly cleaved mica and dried overnight at room temperature. Images were obtained by a Digital Instruments nanoscope IIIa Multimode SFM (Digital Instruments Inc., Santa Barbara, CA) in air at room temperature using the tapping mode.

ζ -potential measurement

The ζ -potentials of BSA microcapsules were measured at different pHs by a Zetasizer Nanoinstrument Nano Z equipment. The pH was adjusted by 0.1 M NaOH or HCl. Each value was averaged from three parallel measurements.

Results and discussion

Protein multilayer built up on planar substrate

The reaction of GA with diverse proteins has been extensively studied and the reaction is pH-dependent [35]. Jansen et al. [36] showed that the optimum pH for GA

insolubilization varies from proteins to proteins. Specially, the pH for the most rapid insolubilization of BSA was found to be nearly the same as its isoelectric point (pI; pH 4.7). The existence of an optimum pH suggests the important role of the protein charge on the intermolecular cross-linking which is required for the formation of insoluble protein layer. The charge on the protein may regulate cross-linking, which is maximal when the repulsive charges are minimal. One more recent study also confirmed that shielding the electrostatic repulsion is necessary for the successful LbL assembly of like charged polyelectrolyte [37]. So here the pH 4.7 (the pI of BSA) and relatively high ionic strength (0.5 M NaCl) were used for the construction of BSA multilayers. First, the BSA multilayers were assembled on silicon wafer for the sake of monitoring the film growth by ellipsometry. Figure 1 shows that the film thickness increases steadily in a linear way with the increase of layer number. The average increment of one BSA layer is about 3 nm. The crystal structure of albumin reveals a heart-shape molecule that can be approximated to an equilateral triangle with sides of ~8 nm and a depth of ~3 nm [31]. Therefore, here each absorbed BSA layer is more likely a monolayer. These results confirm that mediated via GA, the BSA multilayers can be successfully built up on a planar surface and its thickness increment can be controlled at the nanometer scale.

Hollow protein microcapsules

In order to obtain capsules with good integrity, the free-standing multilayers of the microcapsules should be strong enough to resist the osmotic pressure during the core removal process [38, 39]. Therefore, the ten-layer BSA

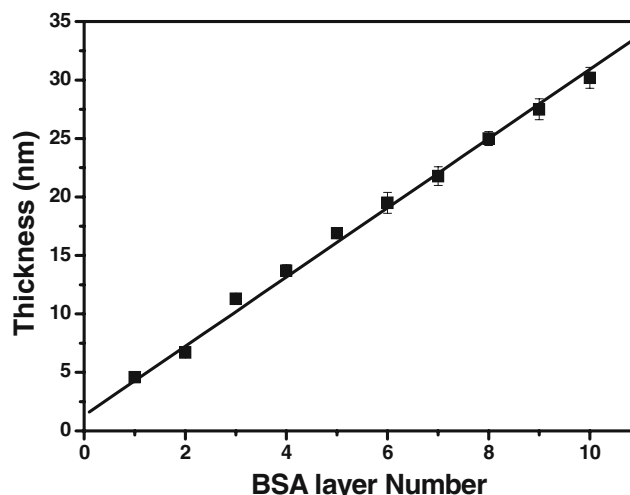
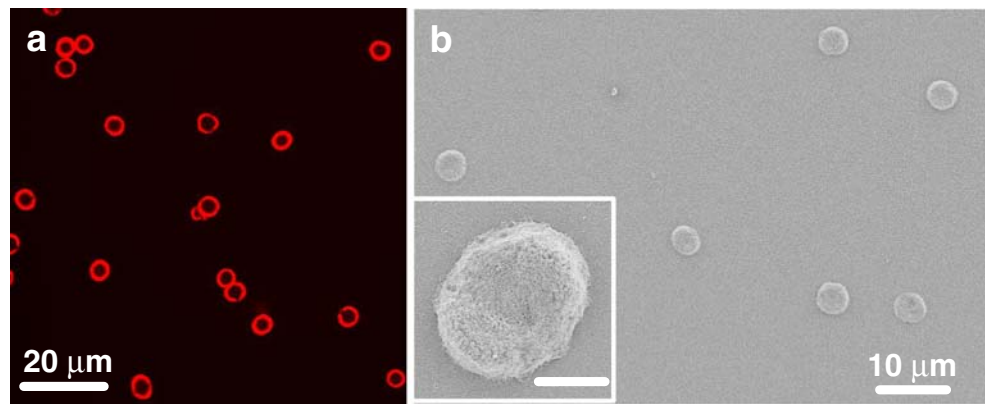


Fig. 1 The thickness of the BSA multilayers formed on the silicon wafer as a function of layer number, determined by ellipsometry. The solid line is a linear fit of the data

Fig. 2 CLSM image (a) and SEM image (b) of the ten-layer BSA hollow microcapsules. The inset of b is a magnified capsule; the scale bar=2 μm



coated particles were further cross-linked with GA for 24 h to stabilize the structure. The post treatment with longer reaction time is necessary because the reaction of GA with lysine residues is progressive with time, probably depending on the accessibility of the amino groups [40, 41]. Then the MnCO_3 templates were removed and the BSA capsules were washed with EDTA solution and water. Visualized under CLSM (Fig. 2a), the obtained microcapsules are well dispersed in water and resemble the shape of their templates as those fabricated by the traditional electrostatic assembly. However, their size shrinks from $7.4 \pm 0.4 \mu\text{m}$ (core size) to $5.1 \pm 0.3 \mu\text{m}$. Size shrinkage after core removal was also observed for polypeptide microcapsules and nanoporous

protein spheres [42, 43]. Molecular relaxation should contribute partially to this phenomenon. Recent studies show that the balance between hydrophobicity and hydrophilicity contributes to surface energy of the capsules, which may cause shrinkage if hydrophobicity dominates, or expansion if the lateral electrostatic repulsion dominates [44].

After evaporation of the water, the hollow capsules collapse (Fig. 2b) to a pancake topology without typical folds and creases often observed in traditional multilayer microcapsules [18]. The SFM images provide more clear visualization (Fig. 3a). Here we make two assumptions for estimating the wall thickness after shrinkage: the thickness of the BSA multilayers assembled on the MnCO_3 particles

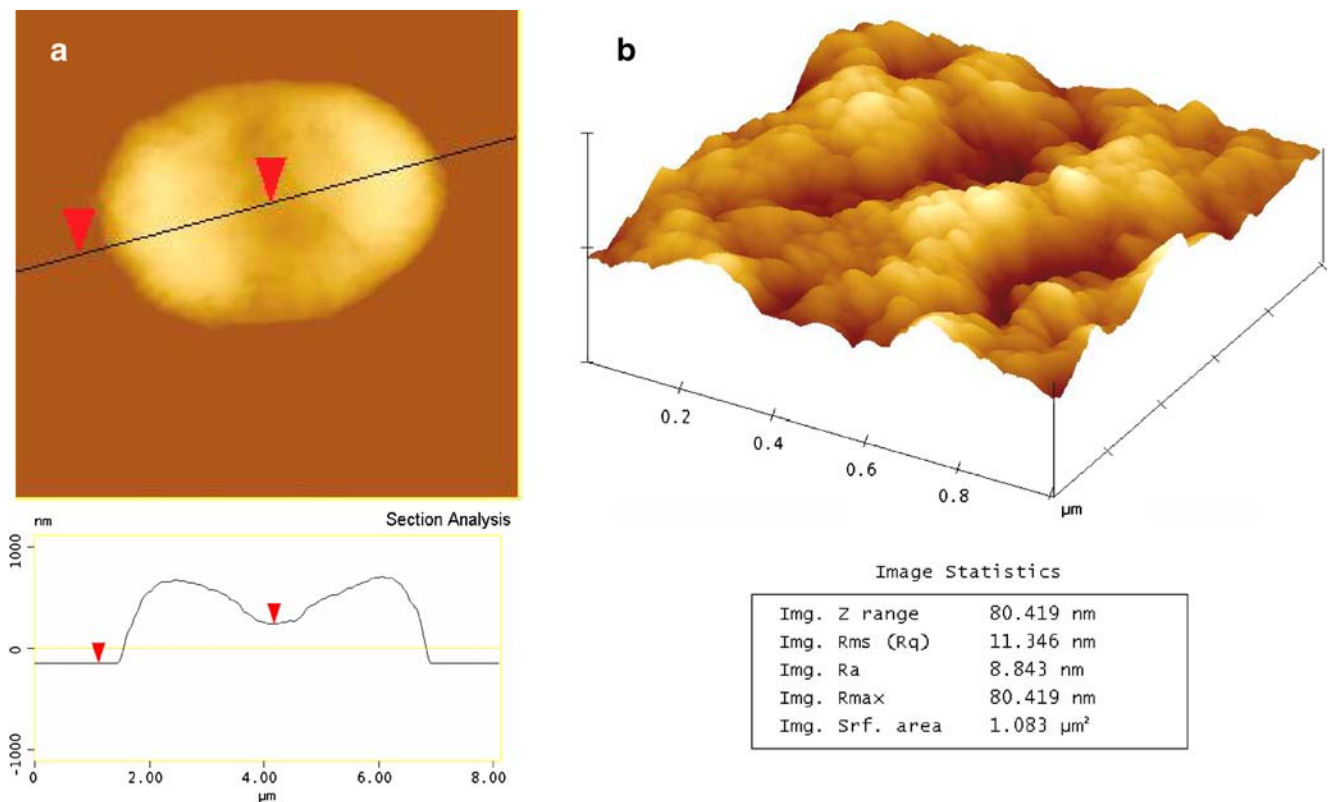


Fig. 3 SFM image (a) of the ten-layer BSA hollow microcapsules. b is a higher magnification of a flat part of the capsule shown in (a)

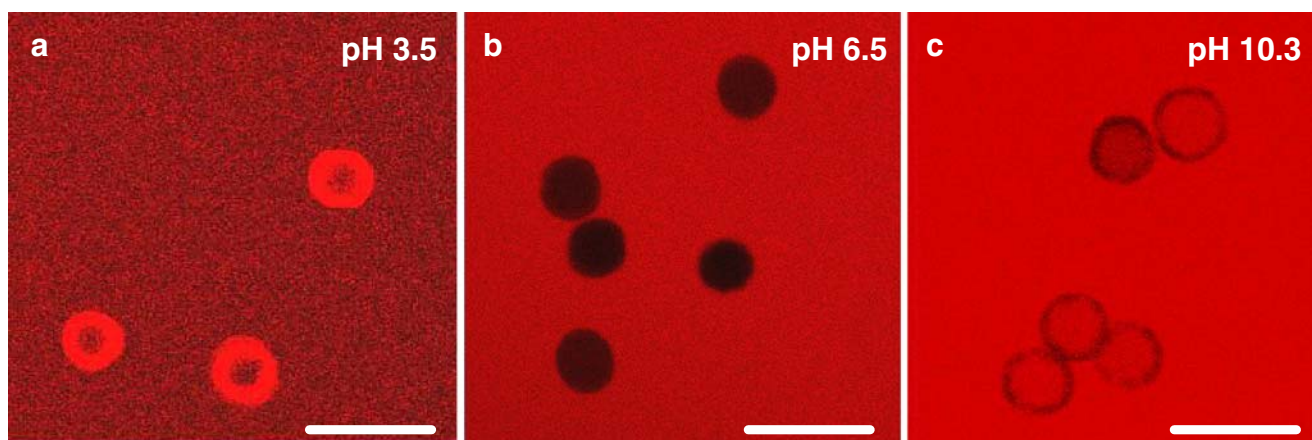


Fig. 4 CLSM images of the ten-layer BSA microcapsules after mixed with TRITC-dextran ($M_w \sim 155$ kDa) for 30 min at different pHs: **a** pH 3.5, **b** pH 6.5 and **c** pH 10.3. The capsules are impermeable to

macromolecules in the pH range of 4–10, while are permeable below pH 4 or above 10. Scale bar = 10 μm

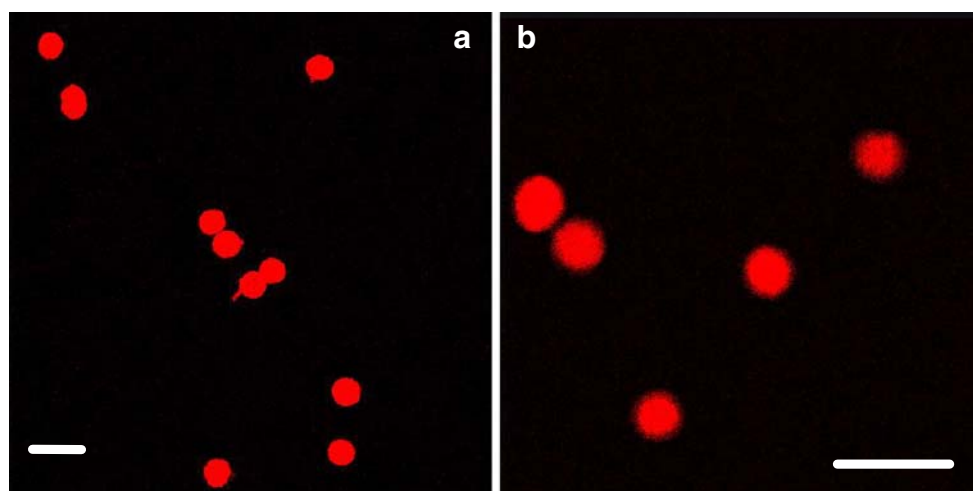
before core removal is equal to that on the planar silicon wafer, and there is no material loss during the capsule shrinkage after core removal, thus the volume of the wall should keep constant in a dry state. Therefore, the thickness of the capsule walls should increase after capsule shrinkage, and the double wall thickness is estimated as ~ 126 nm. This value is far larger than that of the traditional polyelectrolyte multilayers with the same layer number (~ 40 nm) [18]. However, it is still smaller than the apparent double wall thickness (~ 300 nm) measured from the minimum height of the capsules in the SFM images, indicating that more materials are adsorbed onto the rough MnCO_3 particles and the capsules may not be completely collapsed and flattened. These facts can explain the morphology difference between the BSA microcapsules and the polyelectrolyte microcapsules observed from the SEM and AFM images. The capsule surface shows a rough morphology with a ridge-like structure (root-mean-squared roughness (RMS) on $1 \mu\text{m} \times 1 \mu\text{m}$ was 11.3 nm; Fig. 3b). Grains and domains ranging from tens to hundreds of nanometers also can be

seen. We suppose that the shrinkage of the capsule should greatly influence the surface morphology to induce the wrinkled and rough structure.

pH-controlled permeability of the protein microcapsules

The permeability of the hollow BSA capsules is particularly interesting due to its close relationship with diverse applications. Thus the permeation of low-molecular-weight dyes as well as macromolecules was investigated by CLSM after incubation for 30 min. It was found that the BSA microcapsules are permeable for low-molecular-weight dyes, such as Rd6G (data not shown). However, the situation is different for TRITC-dextran with a molecular weight of 155 kDa. Representative CLSM images obtained at different pHs are shown in Fig. 4. At acidic and alkaline conditions, e.g., pH 3.5 and 10.3, respectively (Fig. 4a,c), the capsules have the same fluorescence intensity inside as the bulk solution, implying that the dextran can penetrate inside. By sharp contrast, at neutral pH (pH 6.5), the

Fig. 5 CLSM images of the BSA microcapsules loaded with TRITC-dextran ($M_w \sim 155$ kDa) through the pH-controlled permeability switching protocol. The capsules were incubated with TRITC-dextran solution at **(a)** pH 3.5, **(b)** pH 10.3 for 30 min and washed after the pH was adjusted to 6.5. Scale bar = 10 μm



interiors of the capsules remain dark at least for 30 min (Fig. 4b), implying that the dextran can not penetrate inside. This image reveals also that most of the capsules preserve their good integrity after core removal. We checked the pH range of 1–12. The transition points of permeability for macromolecules were found around pH 4 and pH 10. In other words, the pH values for the TRITC-dextran to permeate inside are <4 and >10 . It is worth mentioning that the size of the capsule remained constant ($5.1 \pm 0.3 \mu\text{m}$) at pH below 10, while increased to $6.1 \pm 0.3 \mu\text{m}$ at pH above 10. Both of the pH-responsive permeability and swelling are reversible.

The pH-responsive properties have been reported for different multilayer capsules [25, 45–50]. It has been suggested that the change of the polyelectrolyte charges upon pH variation might induce reorganization of the wall structure or loosen the polyelectrolyte networks, enabling the macromolecules to penetrate [25, 45, 50]. The lateral electrostatic repulsion between the same net charges resulting from the pH change is considered as the main driving force to induce a swelling of the whole structure [46–48]. Moreover, the attraction of counterions by the net charge may increase the local osmotic pressure and contribute to the swelling effect [48]. Generally, the swelling of the capsules is accompanied by the increase of permeability [46, 51]. This mechanism should be applicable to the swelling and the enhanced permeability of the BSA capsules at pHs above 10. Albumins are characterized by a high content of charged amino acids, such as aspartic and glutamic acids, lysine, and arginine [30, 31]. GA cross-linking only modifies the amine group of lysine [32], so the carboxyls still exist and are almost fully charged at pH above 10 to gain a net negative charge in the capsule walls. To confirm this point, the ζ -potentials of the BSA hollow capsules were investigated at different pHs. The results showed that at pH 10, the capsules are more negatively charged ($-23.8 \pm 3.5 \text{ mV}$) than that at pH 6.5 ($-13.3 \pm 1.9 \text{ mV}$). The result implies also although the capsules possess net negative charge at neutral pH, the value is not high enough to cause the swelling of the capsules.

Albumin was reported to undergo a major reversible conformation change with changes of pH [30, 31]. In a previous study [23], a permeability increase of human serum albumin (HSA)/lipids microcapsules was also observed at pH below 4.8. The expanded conformation of HSA is believed to disorder the structure of lipid bilayers, thus enhancing the permeation of macromolecules. To investigate whether the conformation change near pH 4 induces the permeability change or not, we deposited the BSA multilayers on the inner surface of a quartz cell and filled the cell with water with pHs of 3.5, 4, and 4.5 then measured the circular dichroism (CD) spectra. No obvious difference was found between these spectra (data not

shown). We measured the ζ -potential of the BSA microcapsules at pH 4 also, and found a value of $-1.4 \pm 1.2 \text{ mV}$. Therefore, at least from the viewpoint of charge interaction, we believe that the microstructure of the microcapsules should have been similarly altered as that in the basic solution, since the absolute variable values at lower and higher pH are almost same ($\sim 10 \text{ mV}$).

The ability of reversible permeability switching provides a facile and effective way to control the loading and release of various macromolecules. For example, the capsules were incubated in TRITC-dextran ($M_w \sim 155 \text{ kDa}$) solution at pH 3.5 or 10.5 for 30 min, and then the pH value was adjusted to 6.5. After removal of the bulk solution by centrifugation and washing, TRITC-dextran was successfully loaded into the microcapsules as verified by the strong fluorescence from the capsule interiors (Fig. 5). The encapsulated macromolecules did not leak out at least for 2 weeks (data not shown).

Conclusion

We describe here the fabrication of hollow BSA microcapsules through a GA-mediated covalent LbL assembly method and subsequent core removal. The linear growth of the BSA multilayers as a function of layer number was monitored by ellipsometry, illustrating that the increment of the thicknesses can be controlled in a nanometer scale. These BSA capsules exhibit reversible pH-responsive permeability. They are permeable for macromolecules at pH below 4 or above 10, while are impermeable in between. The permeability transition at pH 10 is attributed to the swelling of the capsules as a result of charge repulsion. Using this feature, macromolecules can be loaded and sealed for at least for 2 weeks. This method can be extended to other proteins and enzymes also, which are not only biocompatible but also bioactive. The protein microcapsules with pH-tunable permeability are relevant to many applications, especially those related with drug release.

Acknowledgments We thank Prof. J. C. Shen for his continuous support and stimulating discussions. A. Heilig and Dr. G. Zhang are greatly acknowledged for their assistance in SFM and SEM measurements, respectively. W.J. Tong and C.Y. Gao thank the Max-Planck Society for a visiting scientist grant. This study is financially supported by China Postdoctoral Science Foundation (Nos. 20070421171), the Natural Science Foundation of China (Nos. 20434030, 20774084) and the National Science Fund for Distinguished Young Scholars of China (No. 50425311).

Open Access This article is distributed under the terms of the Creative Commons Attribution Noncommercial License which permits any noncommercial use, distribution, and reproduction in any medium, provided the original author(s) and source are credited.

References

1. Arshady R (1990) *J Control Release* 14:111
2. Lee TK, Sokoloski TD, Royer GP (1981) *Science* 213:233
3. Longo WE, Iwata H, Lindheimer TA, Goldberg EP (1982) *J Pharm Sci.-US* 71:1323
4. Chen Y, Willmott N, Anderson J, Florence AT (1987) *J Pharm Pharmacol* 39:978
5. Knepp WA, Jayakrishnan A, Quigg JM, Sitren HS, Bagnall JJ, Goldberg EP (1993) *J Pharm Pharmacol* 45:887
6. Latha MS, Rathinam K, Mohanan PV, Jayakrishnan A (1995) *J Control Release* 34:1
7. Willmott N, Magee GA, Cummings J, Halbert GW, Smyth JF (1992) *J Pharm Pharmacol* 44:472
8. Heelan BA, Corrigan OI (1998) *J Microencapsul* 15:93
9. Lee SJ, Rosenberg M (1999) *J Control Release* 61:123
10. Weber C, Coester C, Kreuter J, Langer K (2000) *Int J Pharm* 194:91
11. Gomez A, Bingham D, de Juan L, Tang K (1998) *J Aerosol Sci* 29:561
12. Suslick KS, Grinstaff MW (1990) *J Am Chem Soc* 112:7807
13. Grinstaff MW, Suslick KS (1991) *Proc Nat Acad Sci U.S.A.* 88:7708
14. Lu G, An ZH, Tao C, Li JB (2004) *Langmuir* 20:8401
15. Decher G (1997) *Science* 277:1232
16. Decher G, Hong JD, Schmitt J (1992) *Thin Solid Films* 210:831
17. Caruso F, Caruso RA, Möhwald H (1998) *Science* 282:1111
18. Donath E, Sukhorukov GB, Caruso F, Davis SA, Möhwald H (1998) *Angew Chem Int Edit* 37:2202
19. Peyratout CS, Dähne L (2004) *Angew Chem Int Edit* 43:3762
20. Tiourina OP, Sukhorukov GB (2002) *Int J Pharm* 242:155
21. Balabushevich NG, Tiourina OP, Volodkin DV, Larionova NI, Sukhorukov GB (2003) *Biomacromolecules* 4:1191
22. An ZH, Tao C, Lu G, Möhwald H, Zheng SP, Cui Y, Li JB (2005) *Chem Mater* 17:2514
23. An ZH, Möhwald H, Li JB (2006) *Biomacromolecules* 7:580
24. Tong WJ, Gao CY, Möhwald H (2005) *Chem Mater* 17:4610
25. Tong WJ, Gao CY, Möhwald H (2006) *Macromolecules* 39:335
26. Tong WJ, Gao CY, Möhwald H (2006) *Macromol Rapid Comm* 27:2078
27. Tong WJ, Gao CY, Möhwald H (2008) *Polym Advan Technol* DOI 10.1002/pat.1040 (in press)
28. Duan L, He Q, Yan XH, Cui Y, Wang KW, Li JB (2007) *Biochem Bioph Res Co* 354:357
29. Hou SF, Wang JH, Martin CR (2005) *Nano Letters* 5:231
30. Peters T (1985) *Adv Protein Chem* 37:161
31. Carter DC, Ho JX (1994) *Adv Protein Chem* 45:153
32. Rubino OP, Kowalsky R, Swarbrick J (1993) *Pharm Res* 10:1059
33. Antipov AA, Shchukin D, Fedutik Y, Petrov AI, Sukhorukov GB, Möhwald H (2003) *Colloid Surface A* 224:175
34. Tong WJ, Gao CY (2007) *Colloid Surface A* 295:233
35. Habeeb AFS, Hiramoto R (1968) *Arch Biochem Biophys* 126:16
36. Jansen EF, Tomimats Y, Olson AC (1971) *Arch Biochem Biophys* 144:394
37. Johnston APR, Read ES, Caruso F (2005) *Nano Letters* 5:953
38. Gao CY, Moya S, Donath E, Möhwald H (2002) *Macromol Chem Phys* 203:953
39. Gao CY, Moya S, Lichtenfeld H, Casoli A, Fiedler H, Donath E, Möhwald H (2001) *Macromol Mater Eng* 286:355
40. Bullock GR (1984) *J Microsc-Oxford* 133:1
41. Ottesen M, Svensson B, Trav CR (1971) *Lab Carlsberg* 38:171
42. Yu AM, Wang YJ, Barlow E, Caruso F (2005) *Adv Mater* 17:1737
43. Wang YJ, Caruso F (2006) *Adv Mater* 18:795
44. Köhler K, Möhwald H, Sukhorukov GB (2006) *J Phys Chem B* 110:24002
45. Antipov AA, Sukhorukov GB, Leporatti S, Radtchenko IL, Donath E, Möhwald H (2002) *Colloid Surface A* 198:535
46. Déjugnat C, Haložan D, Sukhorukov GB (2005) *Macromol Rapid Comm* 26:961
47. Déjugnat C, Sukhorukov GB (2004) *Langmuir* 20:7265
48. Mauser T, Déjugnat C, Sukhorukov GB (2004) *Macromol Rapid Comm* 25:1781
49. Shutava T, Prouty M, Kommireddy D, Lvov Y (2005) *Macromolecules* 38:2850
50. Sukhorukov GB, Antipov AA, Voigt A, Donath E, Möhwald H (2001) *Macromol Rapid Comm* 22:44
51. Gao CY, Möhwald H, Shen JC (2004) *Chemphyschem* 5:116